Synergistic Effect of Vermiculite on the Intumescent Flame Retardance of Polypropylene

Qiang Ren,[1,2] Yong Zhang,[1] Jian Li,[2] Jin Chun Li[2]

[1]*State Key Laboratory of Metal Matrix Composites, School of Chemistry and Chemical Technology, Shanghai Jiao Tong University, Shanghai 200240, China*
[2]*Key Laboratory for Polymer Materials, Department of Materials Science and Engineering, Changzhou University, Changzhou, Jiangsu 213164, China*

Received 16 February 2010; accepted 27 July 2010
DOI 10.1002/app.33113
Published online 9 November 2010 in Wiley Online Library (wileyonlinelibrary.com).

ABSTRACT: Synergistic effects of the natural clays unexfoliated vermiculite (VMT), exfoliated vermiculate (EVMT), and montmorillonite (MMT) on the intumescent flame retardance of polypropylene were investigated systematically with the usual fire testing methods. The limiting oxygen index (LOI) of flame-retardant polypropylene (FRPP) filled with 30 wt % intumescent flame retardants (IFRs) composed of ammonium polyphosphate and pentaerythritol were increased from 30 to 33 vol % for VMT and MMT and to 36 vol % for EVMT when 1 wt % IFR was substituted for clay. The synergistic effectivities calculated on the basis of increases in the LOI values were 1.4 for VMT, 1.3 for MMT, and 1.6 for EVMT. Cone calorimetry also revealed the existence of a synergistic effect. EVMT had the best performance for lowering the peak values of the heat release rate and smoke production rate. The thermogravimetric analysis results show that EVMT had the best performance for increasing the char residue of FRPP higher than 650°C compared with VMT and MMT. The high content of iron and the small particle size of EVMT may have been responsible for its high synergistic effect at a low filling level. No remarkable variations of the diffraction peaks were observed in the X-ray diffraction patterns of the original clay and the clay in FRPP. All of the formulations, with or without clay, exhibited small variations in the mechanical properties. © 2010 Wiley Periodicals, Inc. J Appl Polym Sci 120: 1225–1233, 2011

Key words: clay; flame retardance; intumescence; poly(propylene) (PP)

INTRODUCTION

Polypropylene (PP) is one of the most widely used polymers for many applications. PP will burn easily once it is exposed to fire because of its chemical structure. The utility of intumescent flame retardants (IFRs) in polyolefin have attracted extraordinary attention in recent decades.[1,2] It is the most promising approach for achieving halogen-free flame retardance, a lower density, and good processability.[1] All intumescent systems generally include three basic ingredients: an acid source, a charring agent, and a blowing agent.[3] An acid source, such as ammonium polyphosphate (APP), can produce acidic species that act as catalysts at critical temperatures. Charring agents are mainly polyhydric compounds, such as pentaerythritol (PER) and its derivatives (dipentaerythritol and tripentaerythritol), which can form carbonaceous materials under acid catalysis. A blowing agent can release a large amount of gases, which cause the char to swell, and so the heat conductivity of the char decreases, and the insulation of the substrate is enhanced. APP can also act as a blowing agent because it can give off ammonia and water during pyrolysis and esterification. The flame-retardant mechanism is based on the charred layer acting as a physical barrier; this slows the heat and mass transfer between the gas and condensed phases.

To enhance the intumescent flame retardance of polymeric materials, various compounds, such as aluminosilicate species (including most natural clays),[4–12] zinc borate,[13,14] and other metallic compounds,[15–18] have been used as synergists in IFR systems.[2] Clay has been the most widely studied because of its low cost and some of its benefits to the properties and processing of the filled polymers.[2] The effects of various clays on IFR materials depend on chemical compositions and dispersion states of the clays in the polymer matrix.[4,9,12] Among all of the aluminosilicate fillers, synthetic zeolite is one of the species that has showed the best synergistic effects in the polyethylenic polymer matrix.[19] Another kind of important species is layered aluminosilicates, such as montmorillonite (MMT), which can be intercalated or exfoliated in the polymer matrix to form nanocomposites with lowered peak

Correspondence to: Y. Zhang (yong_zhang@sjtu.edu.cn).
Contract grant sponsor: National Natural Science Foundation of China; contract grant numbers: 50803035, 50773036.
Contract grant sponsor: Shanghai Leading Academic Discipline Project; contract grant number: B202.

values of the heat release rate (pHRR's) and increased UL 94 rating.[6–8,11] Vermiculite is also a 2 : 1 layered aluminosilicate with a cation exchange capacity similar to that of MMT, but it is characterized by its large crystals.[20] So it is generally introduced into the polymer matrix like MMT, with intercalated or exfoliated states, to prepare nanocomposites.[21–23] Another unusual property of vermiculite is its expansion into wormlike pieces under temperatures above about 300°C;[24] this is where the name *vermiculite* comes from. In the expansion process (i.e., *exfoliation*), the increase in the bulk volume of commercial grades is 8–12 times, but individual flakes may exfoliate as much as 30 times.[24] Exfoliated vermiculite (EVMT) has a loose character, is easily ground into fine particles, and has been widely used in high-temperature insulation, refractory insulation, and the fireproofing of structural steel, pipes, and wallboard.[25,26] The addition of EVMT as a synergist into polymeric IFRs has not been reported up to this point. On the other hand, because unexfoliated vermiculite (VMT) and IFR all can be expanded in a similar temperature range, the combination of VMT with IFR may bring an enhancement of intumescent flame retardance. The comparison of the effects of VMT and EMVT on the intumescent flame retardance of PP is an interesting idea, and it was investigated in this study. For comparison, the synergistic effect of the frequently studied clay species MMT was also examined in this study.

EXPERIMENTAL

Materials

The PP we used was T30S (melt index = 3.8 g/10 min, 230°C, 2.16 kg), which was produced by Sinopec Zhenhai Petrochemical Industry Co., Ltd. (Zhenhai, Zhejiang Province, China) Maleated polypropylene (PP-*g*-MAH; MA content = 1.0 wt %) was provided by Sunrising Engineering Plastics Co. (Shanghai, China). APP, with the brand name AP422 [P (%) = 31.5 wt %], was from Clariant Co. (Huerth, Germany). PER of a purity higher than 98% was commercially obtained from Shanghai Chemical Reagent Co. (Shanghai, China). Original VMT, with a particle size of 35.5 μm, and EVMT, with a particle size of 1.4 μm, was provided by Zhongke Mining Co., Ltd. (Lingshou County, Henan Province, China). MMT, with particle size of 4.1 μm, was provided by Fenghong Clay Chemicals Co., Ltd. (Anji County, Zhejiang Province, China).

Measurement of the VMT expansion ratio

VMT powder (4 mL) was loaded into a 10-mL quartz measuring cylinder and then placed in a muffle furnace. The temperature of the muffle furnace was increased from ambient temperature to 700°C at a heating rate of 20°C/min and then cooled so that we could observe the bulk volume variation of VMT.

Compounding and specimen preparation

APP, PER, and clay at the desired proportions were ground with a pestle in a mortar for 10 min to obtain a homogeneous mixture. The weight ratio of APP to PER in IFR was fixed at 3 : 1. In this study, all formulations were based on the weight fraction. The total loading of additives, including APP, PER, and clay, was 30 wt %. Various contents of clay in the range 0.5–7 wt %, were used to substitute APP and PER into the formulations. PP-*g*-MAH (10 wt %) was used as a compatibilizer between IFR and PP. Flame-retardant polypropylene (FRPP) was prepared by the compounding of PP, PP-*g*-MAH, and additives in a Haake Rheomix mixer (Karlsruhe, Germany) at 190°C with a rotation speed of 60 rpm for 10 min. After mixing, the sample was hot-pressed at 190°C with a pressure of 10 MPa to obtain sheets with the required dimensions.

Combustion tests

The limiting oxygen index (LOI) was measured according to ASTM D 2863 on sheets with dimensions of 120 × 6.5 × 3 mm^3. The apparatus used was an HC-2 oxygen index meter from Jiangning Analysis Instrument Co. (Nanjing, China).

The vertical combustion test was carried out according to the UL 94 test from ASTM D 3801 on a CFZ-2 type instrument from Jiangning Analysis Instrument Co. (Nanjing, China). The specimen used had dimensions of 120 × 13 × 3 mm^3.

Cone calorimetry tests were performed according to ASTM D 1354 on an FTT standard cone calorimeter from Fire Testing Technology Co., Ltd. (West Sussex, UK). A specimen with dimensions of 100 ×100 ×3 mm^3 was wrapped in aluminum foil and exposed horizontally to an external heat flux of 50 kW/m^2.

Thermogravimetric analysis (TGA)

TGA and derivative thermogravimetry (DTG) were carried out on an SDTQ-600 thermogravimetric analyzer of TA Instruments (New Castle, Delaware) under an air atmosphere in the temperature range 50–800°C at a heating rate of 20°C/min. Samples (ca. 10 mg) were positioned in open aluminum oxide pans.

Mechanical property measurements

The tensile properties of the materials were determined according to ASTM D 638 with dumbbell-shaped samples with dimension of 75 × 1 × 20 mm^3

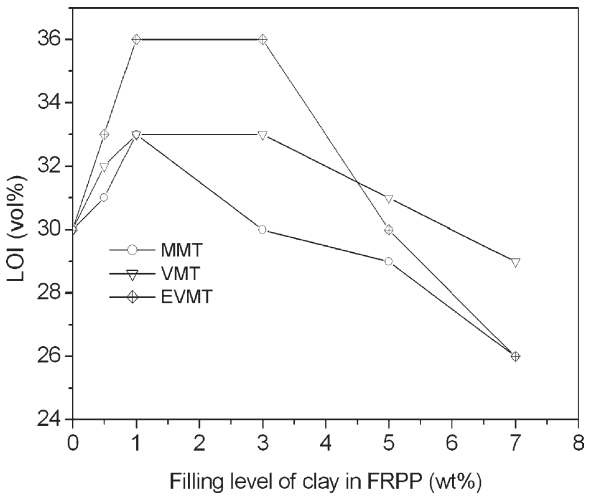

Figure 1 LOI values versus the filling level of clay in FRPP.

at a speed of 50 mm/min on a WDT-5 tensile tester from Kai Qiang Li Mechanical Co. (Shenzhen, China).

The Izod notched impact strength was determined according to ASTM D 256 with samples with dimensions of 12.7 × 64 × 3 mm^3 on an XJU-22 impact tester from Chengde Testing Machine Co. (Hebei Province, China). The depth of the notch was 2.5 mm, and the radius of the notch tip was 0.25 mm.

X-ray diffraction (XRD) characterization

The XRD spectra were recorded in the 2 θ range 2–10° with a Rigaku D/max 250 diffractometer [λ(Cu Kα) = 1.5406 Å, 40 kV, 100 mA] (Tokyo, Japan) at a scanning rate of 2°/min.

Energy-dispersive spectrometry (EDS) analysis

EDS was performed on an EX-54175JMU JEOL microanalyzer (Tokyo, Japan) attached to a JEOL JSM-6360LA scanning electron microscope (Tokyo, Japan). A powder sample was pressed into a slice with a flat surface and was then sputter-coated with a thin layer of platinum before analysis.

RESULTS AND DISCUSSION

Synergistic effectivity (SE) calculated from LOI values

The addition of 30 wt % IFR increased the LOI value of PP from 18 to 30 vol % (Fig. 1). The substitution of part of IFR by clay further improved the flame retardance of FRPP, as revealed by the increase in the LOI value. The incorporation of 1 wt % VMT, EVMT, and MMT led to the highest LOI values of 33, 36, and 33 vol %, respectively. For FRPP containing VMT and EVMT, the LOI values had a plateau between clay filling levels in the range 1–3 wt %. For FRPP containing MMT, the LOI value began to decrease after the maximum value of 33 vol % at the 1 wt % filling level. The increase in the LOI values of FRPP in the presence of EVMT was remarkable compared with MMT in our study and others.[6,11] Another silicate with a high synergistic effect in IFR is zeolite, which can make the LOI values jump from 30 to 39 vol % when 1.5 wt % of zeolite is added in an intumescent flame-retardant terpolymer composed of ethylene (91.5%), butyl acrylate (5%), and maleic anhydride (3.5%). However, the LOI value only increased from 25 to 27 vol % for nonpolar polyethylene.[27] Generally, aluminosilicate species can play a catalytic role in the oxidative dehydrogenation–crosslinking–charring process of PP, even in microcomposites.[28] The interaction of clay with APP can produce aluminosiliconphosphate species with active catalytic roles for promoting the synthesis of a protective carbonaceous layer with a high thermal stability.[19] The particle size of EVMT (1.4 μm) was much smaller than that of VMT (35.5 μm), which benefited the interaction of clay with IFR and PP. So EVMT had much better performance for increasing the LOI values of FRPP at a low clay filling level (<5 wt %). On the other hand, the unusual expandable properties of VMT when it is exposed to heat need to be considered because the high fire shrinkage of some clay particles may be initiators for the development of cracks in the charred layer and the loss of a protective shield.[4] The expansion behavior can be determined in a high-temperature thermal mechanical dilatometer,[29] which was not available in our laboratory. The rough manner of measuring the expansion ratio of VMT in a quartz measuring cylinder by thermal treatment revealed that the bulk volume of VMT after expansion increased from 4 to 5.6 mL; this indicated a rough expansion ratio of 1.4. The expansion ratio was not accurate but could have reflected the thermal expansion behavior of VMT. The simultaneous expansion of VMT and IFR could have resulted in a thicker, compacter, and more thermally stable protective shield and, thus, high LOI values. The LOI value for FRPP containing VMT decreased slowly and was

TABLE I
FR EFF and SE of the FRPP System

Sample	Synergist	ΔLOI	EFF[a]	SE[a]
PP and 30% IFR		12	1.7	
PP, 29% IFR, and 1% MMT	MMT	15	2.2	1.3
PP, 27% IFR, and 3% VMT	VMT	15	2.4	1.4
PP, 27% IFR, and 3% EVMT	EVMT	18	2.8	1.6

[a] For a specific formulation with a synergist: $EFF = \frac{\Delta LOI}{P\%100} = \frac{LOI-18}{P\%100}$, $SE = \frac{EFF}{1.7}$

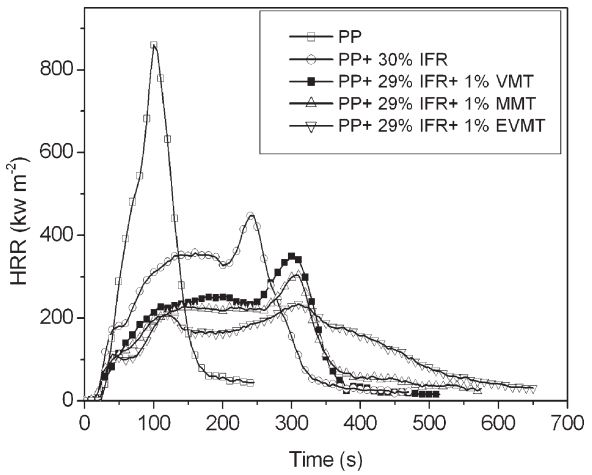

Figure 2 HRR values of PP and FRPP versus the time during combustion.

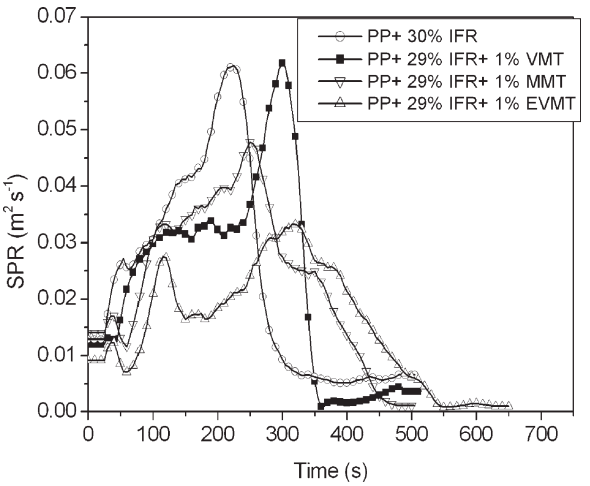

Figure 3 Smoke production rate values of FRPP versus the time during combustion.

higher than those of FRPP containing EVMT or MMT when the clay filling level exceeded 5 wt % (Fig. 1). The less sensitive dependence of the LOI values on the high filling level of VMT compared with MMT, EVMT, and zeolite[27] indicated that VMT itself exhibited some flame-retardant role and did not only perform as a synergist. However, the flame-retardant role of VMT only became remarkable when the filling level was higher than 5%. The *weight flame-retardant effectivity* (EFF) is defined as the increase of LOI for 1 wt % of the flame-retardant element.[30] The flame-retardant element was phosphorus in this study. SE is defined as the ratio of EFF of the flame-retardant additive plus the synergist to that of the additive without the synergist.[30] The formulation with the highest LOI values and the highest filling level of clay was considered the optimal one because clay is cheaper than IFR. EFF and SE were calculated on the basis of the optimal formulation and are shown in Table I. For vertical combustion testing, FRPP with 30% IFR reached a UL 94 V0 rating. FRPPs in the presence of 0.5–7 wt % VMT, 0.5–3 wt % EVMT, or MMT, shown in Figure 1, all reached a UL 94 V0 rating. FRPP with 5 or 7 wt % EVMT or MMT did not self-extinguish after ignition and did not reach a UL 94 vertical combustion rating.

Cone calorimetry tests

Cone calorimetry is often used to directly evaluate the fire safety properties of materials in different fire conditions. The combustion of virgin PP exhibited a single high pHRR (858 kW/m^2) at a combustion time of 100 s. The whole material burned completely within 3 min (Fig. 2 and Table II). The incorporation of 30 wt % IFR in PP delayed the combustion process with a 48% reduction of pHRR compared with virgin PP, and the time for the peak heat release rate (t_{pHRR}) was prolonged to 245 s. However, the time to ignition (T_{ign}) also decreased slightly. An even lower pHRR was observed when 1 wt % clay was added. MMT had a better performance than VMT for decreasing pHRR but had a worse performance than EVMT. The substitution of 1 wt % IFR by EVMT led to a 73% reduction in pHRR and a 30% reduction in total heat release (THR) compared with the virgin PP. VMT had no obvious effect on the smoke release behavior of FRPP (Figs. 3 and 4 and Table II). MMT decreased the peak value of the smoke production rate (pSPR). EVMT decreased both pSPR and the total smoke production (TSP) of FRPP (Figs. 3 and 4 and Table II). The heat release rate (HRR) curves of FRPP had three peaks; the first

TABLE II
Cone Calorimetry Analysis Data for PP and FRPP

Sample	pHRR (kw/m^2)[a]	t_{pHRR} (s)	T_{ign} (s)	THR (MJ/m^2)	Peak MLR (g s^{-1} m^{-2})	pSPR (m^2/s)	TSP (m^2/kg)
PP	858	100	28	120	14	NM	NM
PP and 30% IFR	446 (48)	245	25	90	9	0.061	1283
PP, 29% IFR, and 1% MMT	304 (65)	305	26	84	6.7	0.048	1324
PP, 29% IFR, and 1% VMT	350 (59)	300	22	79	7	0.062	1295
PP, 29% IFR, and 1% EVMT	234 (73)	310	28	84	5.6	0.033	1100

NM = not measured.
[a] Reduction values (%) are shown in parentheses.

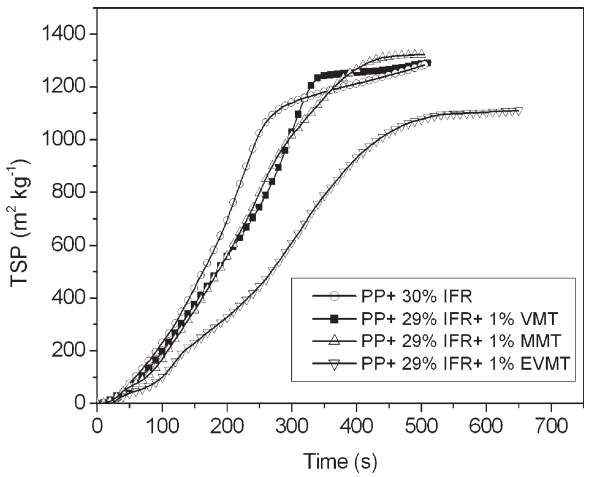

Figure 4 TSP values of FRPP versus the time during combustion.

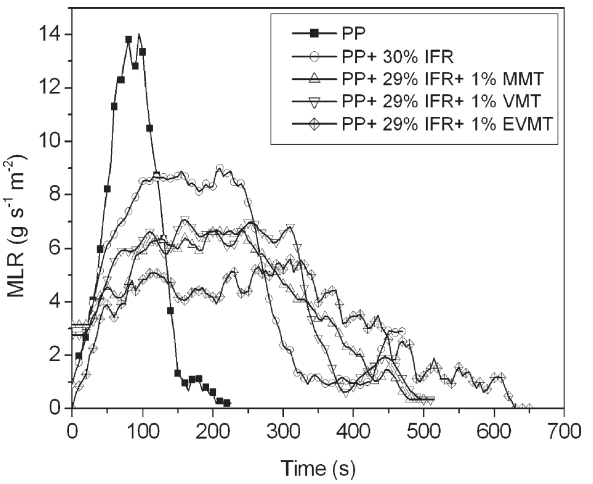

Figure 5 MLR values of PP and FRPP versus the time during combustion.

small peak was assigned to the slight degradation of IFR before interaction with polymeric materials.[14] The second and third peaks were separated by a plateau. The second peak was assigned to the development of the intumescent protective layer, and the third peak was assigned to the degradation of this protective layer.[31] The third pHRR of FRPP without clay was very sharp; this indicated that the shield property of the intumescent layer was not good enough to suppress the thermooxidation degradation of the underlying materials. The third peak of FRPP in the presence of 1 wt % EVMT became flat. The intumescent layer of FRPP in the presence of EVMT underwent a plateau before degradation, and the time to the third pHRR was delayed greatly.

The mass loss rate (MLR; Fig. 5) during the combustion process decreased with the same order of HRR; this indicated that the observed enhancement in flame retardance depended mainly on the condensed-phase process rather than gas-phase process.

The combustion of PP was complete with almost no residue (Fig. 6). The development of an intumescent structure for all FRPP was observed. Cracking occurred in the residual charred layer of FRPP

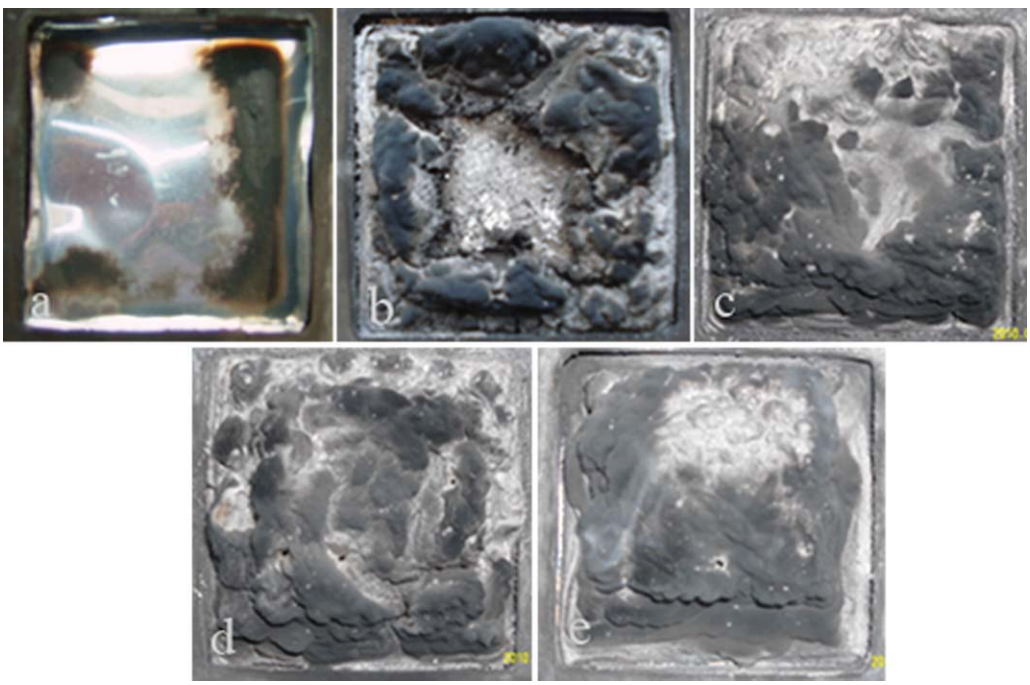

Figure 6 Residues of PP and FRPP after cone calorimetry tests: (a) PP; (b) PP and 30% IFR; (c) PP, 29% IFR, and 1% VMT; (d) PP, 29% IFR, and 1% MMT; and (e) PP, 29% IFR, and 1% EVMT. [Color figure can be viewed in the online issue, which is available at wileyonlinelibrary.com.]

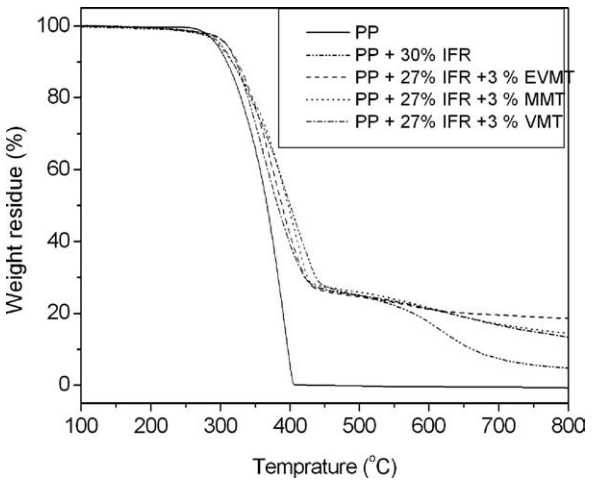

Figure 7 Thermogravimetric curves of PP and FRPP.

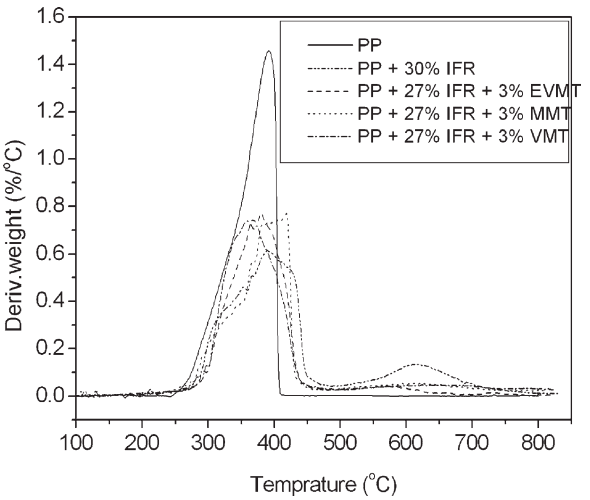

Figure 8 DTG curves of PP and FRPP.

without clay, whereas the layers of FRPP with VMT, MMT, and EVMT expanded well and stayed intact. The thick, compact, and thermally stable charred layer of FRPP in the presence of clay benefited the improvement of the flame retardance.

TGA

TGA is a useful tool for investigating the mechanism of action for flame-retardance improvement of IFR systems containing a synergist because thermooxidative degradation is an important part of the combustion process for polymeric materials. The thermooxidative degradation of PP (Fig. 7 and Table III) occurred in one step at the onset decomposition temperature (T_{onset}; i.e., the 5% weight loss temperature) of 295°C, and complete weight loss occurred at a temperature of 450°C. The addition of 30 wt % IFR in PP slowed the thermal degradation process with higher values of T_{onset} and the 50% weight loss temperature ($T_{-50wt\%}$). The degradation of FRPP occurred in two successive stages. The weight loss rate was fast and corresponded to approximately 70% of the mass loss in the range 250–450°C, in which it is generally accepted that the intumescent process develops. The second step, occurring between 450 and 800°C, was assigned to the degradation of the intumescent structure, probably via oxidative reactions. The addition of 3 wt % VMT, EVMT, and MMT in FRPP had no remarkable effect on the thermal stability of FRPP below 550°C but enhanced the thermal stability of FRPP above 550°C. In the DTG curve of FRPP without clay (Fig. 8), second weight loss peak at 611°C was observed, whereas no obvious weight loss peak was observed in the DTG curves of FRPP with clay. At high temperatures above 650°C, FRPP with EVMT had better thermal stability than those with MMT and EVMT. The results indicate that the intumescent charred layer resulting from the interaction of IFR, PP, and EVMT exhibited longer endurance under severe high-temperature thermooxidative environments; this benefited the improvement of the flame retardance.

Elemental analysis of clay

To determine the cause for the discrepancy of synergistic effects for various clays, elemental analysis of the clays was performed by EDS, and the results are shown in Figure 9 and Table IV. The contents of iron in VMT and EVMT were much higher than that in MMT. The presence of iron ions played a catalytic role in the oxidative dehydrogenation and crosslinking of FRPP to promote char formation and so benefited the flame retardance.[32,33] The high content of iron ions in EVMT may have been responsible for the high synergistic

TABLE III
TGA Data for PP and FRPP

Formulation	T_{onset}	$T_{-50wt\%}$	T_{p1}[a] (°C)	T_{p2}[a] (°C)	Residue (wt %) 400°C	600°C	800°C
PP	295	367	392	–	5.8	0	0
PP and 30% IFR	301	400	389	611	50.3	18.1	4.8
PP, 27% IFR, and 3% MMT	297	398	419	–	48.2	21.7	14.5
PP, 27% IFR, and 3% VMT	309	383	359	–	39.4	21.4	13.4
PP, 27% IFR, and 3% EVMT	308	389	381	–	42.0	21.2	18.7

[a] Temperature according to first and second weight loss peaks on DTG curves.

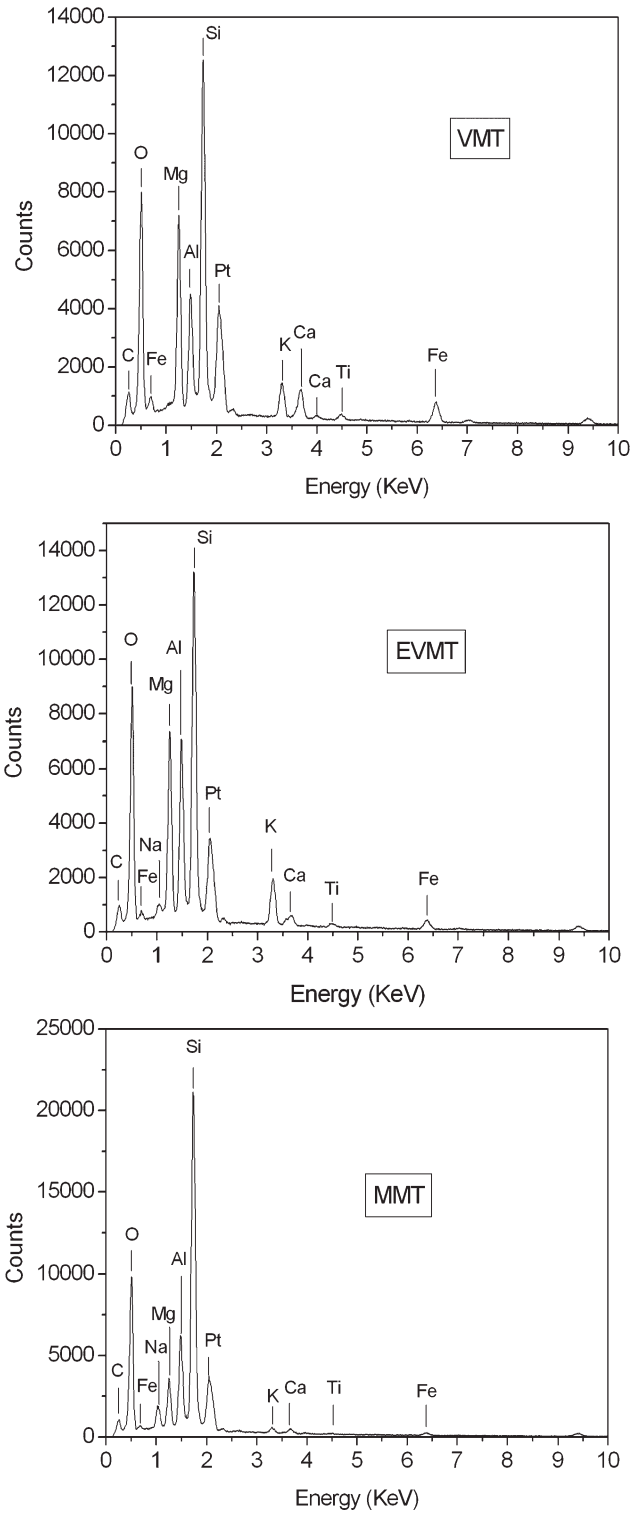

Figure 9 EDS spectra of clay.

effect of EVMT compared with MMT. On the other hand, the iron content of VMT was higher than that of EVMT, but the synergistic effect of VMT was lower than that of EVMT. The possible reason was that the particle size of EVMT (1.4 μm) was much smaller than that of VMT (35.5 μm), which benefited the interaction of clay with IFR and PP. The loss of iron ions for EVMT compared with VMT may have resulted from the ion-exchange treatment during the exfoliation process performed by the manufacturer. It is important to point out that the particle size of VMT could not be lowered further by grinding without destruction to the unexfoliated character of VMT.

XRD characterization of clay in FRPP

MMT and VMT could both be intercalated by the polymer to form nanocomposites. XRD is the most commonly used tool for probing the nanoscale dispersion of layered silicates in polymeric materials.[34] The as-received VMT exhibited characteristic diffraction peaks[35] at 2θ values of 3.26, 6.06, and 7.24° (Fig. 10). The corresponding layer spacings, calculated on the basis of the Bragg equation,[34] were 2.70, 1.46, and 1.22 nm, respectively. The locations of the diffraction peaks of VMT in FRPP were nearly unchanged (Fig. 11). EVMT exhibited only one diffraction peak[36] at a 2θ of 8.82° in the range 2–10°. The location of the diffraction peak of EVMT in FRPP was also unchanged (Fig. 11). All of the results indicate that no intercalation occurred for VMT and EVMT in the melt-compounding process with IFR and PP. For FRPP containing MMT, the diffraction peak shifted from 6.96 to 5.98°, and the corresponding layer spacing increased from 1.20 to 1.48 nm; this indicated that a slight intercalation process occurred. The variation of the layer spacing was very small. On the basis of XRD analysis, we concluded that the addition of the original VMT, EVMT, and MMT to the intumescent FRPP did not result in the formation of nanocomposites. We tried to reveal the dispersion state of clay in FRPP by transmission electron microscopy and scanning electron microscopy, but the presence of a large content of IFR in FRPP (23–30 wt %) disturbed the distinguishability of clay particles. Because IFR in our study and the clay all had hydrophilic characteristics, the small content of clay dispersed mainly in the IFR phase. The flame-retardance improvement mainly resulted from the interaction between clay with IFR. The target of this study was the synergistic effect of IFR and clay rather than the effect of the dispersion state of clay in the PP matrix. If EVMT had been first treated with an organophilic compound, blended with PP, and then compounded with IFR to form FRPP, nanoscale dispersions of EVMT in the PP matrix may have been achieved. This study is in progress and will be reported in a subsequent article.

Mechanical property analysis

The mechanical properties of all of the FRPPs are summarized in Table V. The tensile strength and impact strength exhibit slight increases for some formulations compared to formulations without clay, but the variations were small. All of the FRPPs in

TABLE IV
Element Weight Contents (%) of Different Silicates

Silicate	Clay	O	Na	Mg	Al	Si	K	Ca	Ti	Fe
VMT	8.30	30.5	0.00	11.5	6.98	23.29	4.34	4.1	1.07	9.92
MMT	9.52	33.63	2.47	4.57	8.68	36.34	1.17	1.03	0.23	2.24
EVMT	6.83	32.39	0.81	10.94	11.21	24.52	6.23	1.45	0.71	4.70

Table V were highly filled with 23–30 wt % IFR and 0.5–7 wt % clay. The mechanical properties of FRPP were mainly determined by IFR with large contents rather than clay with small contents. So all of the formulations exhibited small variations in the mechanical properties.

CONCLUSIONS

The substitution of 0.5–7 wt % IFR by VMT, EVMT, and MMT improved the LOI values of FRPPs filled with 30 wt % IFR composed of APP and PER. The formulation with 3 wt % EVMT had the maximum LOI value of 36 vol %, and EVMT had the highest SE of 1.6. EVMT also had the best performance for decreasing the heat release and smoke production parameters of FRPP. TGA demonstrated that the clay had no remarkable effect on the thermal stability of FRPP below 550°C but greatly enhanced the thermal stability of FRPP above 550°C. The formulation with EVMT had the highest char residue at 800°C. EDS revealed that content of iron in VMT and EVMT was much higher than that in MMT. No remarkable variations in the diffraction peaks were observed in the small-angle XRD patterns of the original clay and clay in FRPP. All of the formulations with or without clay exhibited small variations in the mechanical properties.

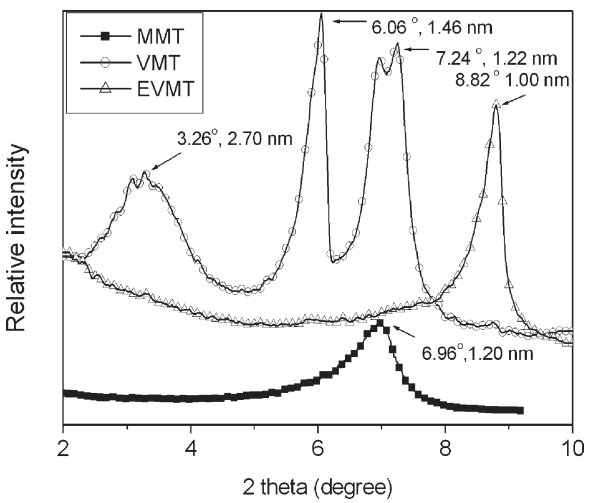

Figure 10 Small-angle XRD patterns of clay.

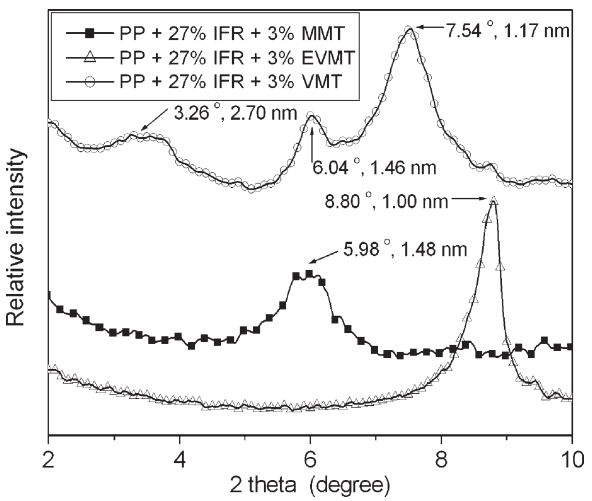

Figure 11 Small-angle XRD patterns of FRPP.

TABLE V
Mechanical Properties of FRPP

Synergist in formulation	Tensile strength (MPa)	Elongation at break (%)	Notched izod impact strength (J/m)
No (i.e. PP+30% IFR)	26.8 ± 0.7	36 ± 3	23.6 ± 2.0
0.5% VMT[a]	27.0 ± 0.8	39 ± 4	23.5 ± 2.0
1% VMT	27.9 ± 0.9	37 ± 2	23.6 ± 2.0
3% VMT	29.3 ± 1.5	35 ± 4	25.6 ± 2.0
5% VMT	28.7 ± 0.8	32 ± 6	27.0 ± 2.0
7% VMT	27.6 ± 0.7	32 ± 2	25.0 ± 1.9
0.5% EVMT	27.2 ± 0.7	24 ± 10	23.5 ± 2.0
1% EVMT	25.7 ± 0.5	26 ± 8	26.0 ± 2.0
3% EVMT	27.7 ± 0.9	28 ± 8	25.7 ± 1.9
5% EVMT	27.8 ± 0.4	23 ± 4	24.3 ± 2.5
7% EVMT	26.2 ± 0.2	21 ± 2	25.6 ± 2.3
0.5% MMT	26.2 ± 0.6	50 ± 10	25.8 ± 2.0
1% MMT	26.5 ± 0.8	49 ± 11	22.7 ± 1.9
3% MMT	27.2 ± 0.3	30 ± 6	24.8 ± 1.6
5% MMT	29.2 ± 1.1	37 ± 1	26.3 ± 2.5
7% MMT	28.6 ± 1.0	37 ± 5	27.4 ± 1.5

[a] The formulation was PP, 29.5% IFR, and 0.5% EVMT. The rest was deduced by analogy.

References

1. Weil, E. A.; Levchik, S. V. J Fire Sci 2008, 26, 5.
2. Bourbigot, S.; Le Bras, M.; Duquesne, S.; Rochery, M. Macromol Mater Eng 2004, 289, 499.
3. Camino, G.; Costa, L.; Trossarelli, L. Polym Degrad Stab 1984, 6, 243.

4. Le Bras, M.; Bourbigot, S. Fire Mater 1996, 20, 39.
5. Dabrowski, F.; Le Bras, M.; Delobel, R.; Gilman, J. W.; Kashiwagi, T. Macromol Symp 2003, 194, 201.
6. Marosi, G.; Marton, A.; Szep, A.; Csontos, I.; Keszei, S.; Zimonyi, E.; Toth, A.; Almeras, X. Polym Degrad Stab 2003, 82, 379.
7. Tang, Y.; Hu, Y.; Wang, S. F.; Gui, Z.; Chen, Z. Y.; Fan, W. C. Polym Int 2003, 52, 1396.
8. Tang, Y.; Hu, Y.; Li, B. G.; Liu, L.; Wang, Z. Z.; Chen, Z. Y.; Fan, W. C. J Polym Sci Part A: Polym Chem 2004, 42, 6163.
9. Morgan, A. B. Polym Adv Technol 2006, 17, 206.
10. Ma, Z. L.; Zhang, W. Y.; Liu, X. Y. J Appl Polym Sci 2006, 101, 739.
11. Liu, Y.; Wang, J. S.; Deng, C. L.; Wang, D. Y.; Song, Y. P.; Wang, Y. Z. Polym Adv Technol, DOI: 10.1002/pat.1502.
12. Chen, Y. J.; Fang, Z. P.; Yang, C. Z.; Wang, Y.; Guo, Z. H.; Zhang, Y. J Appl Polym Sci 2010, 115, 777.
13. Wu, Z. P.; Shu, W. Y.; Hu, Y. C. J Appl Polym Sci 2007, 103, 3667.
14. Fontaine, G.; Bourbigot, S.; Duquesne, S. Polym Degrad Stab 2008, 93, 68.
15. Lewin, M.; Endo, M. Polym Adv Technol 2003, 14, 3.
16. Chen, X. C.; Ding, Y. P.; Tang, T. Polym Int 2005, 54, 904.
17. Li, Y. T.; Li, B.; Dai, J. F.; Jia, H.; Gao, S. L. Polym Degrad Stab 2008, 93, 9.
18. Zhang, P.; Song, L.; Lu, H. D.; Hu, Y.; Xing, W. Y.; Ni, J. X.; Wang, J. Polym Degrad Stab 2009, 94, 201.
19. Bourbigot, S.; Le Bras, M.; Breant, P.; Tremillon, J. M.; Delobel, R. Fire Mater 1996, 20, 145.
20. Letaief, S.; Martin-Luengo, M. A.; Aranda, P.; Ruiz-Hitzky, E. Adv Funct Mater 2006, 16, 401.
21. Tjong, S. C.; Meng, Y. Z.; Hay, A. S. Chem Mater 2002, 14, 44.
22. Tjong, S. C.; Meng, Y. Z. J Polym Sci Part B: Polym Phys 2003, 41, 2332.
23. Zhang, Y.; Han, W.; Wu, C. F. J Polym Sci Part B: Polym Phys 2009, 48, 967.
24. Horacek, H.; Pieh, S. Polym Int 2000, 49, 1106.
25. Kozlowski, R.; Mieleniak, B.; Helwig, M.; Przepiera, A. Polym Degrad Stab 1999, 64, 523.
26. Yadong, Y.; Guangfu, Y.; Xiaowei, C.; Xiangli, G. Key Eng Mater 2007, 336–338, 1753.
27. Bourbigot, S.; LeBras, M.; Delobel, R.; Breant, P.; Tremillon, J. M. Polym Degrad Stab 1996, 54, 275.
28. Zanetti, M.; Camino, G.; Reichert, P.; Mulhaupt, R. Macromol Rapid Commun 2001, 22, 176.
29. James, J. D.; Spittle, J. A.; Brown, S. G. R.; Evans, R. W. Meas Sci Technol 2001, 12, R1.
30. Lewin, M. J Fire Sci 1999, 17, 3.
31. Almeras, X.; Le Bras, M.; Hornsby, P.; Bourbigot, S.; Marosi, G.; Keszei, S.; Poutch, F. Polym Degrad Stab 2003, 82, 325.
32. Zhu, J.; Uhl, F. M.; Morgan, A. B.; Wilkie, C. A. Chem Mater 2001, 13, 4649.
33. Nawani, P.; Desai, P.; Lundwall, M.; Gelfer, M. Y.; Hsiao, B. S.; Rafailovich, M.; Frenkel, A.; Tsou, A. H.; Gilman, J. W.; Khalid, S. Polymer 2007, 48, 827.
34. Sinha Ray, S.; Okamoto, M. Prog Polym Sci 2003, 28, 1539.
35. Xusheng, D.; Daofu, L.; Yuezhong, M. Mater Lett 2006, 60, 1847.
36. Lin, J.; Tang, Q.; Wu, J.; Sun, H. J Appl Polym Sci 2008, 110, 2862.